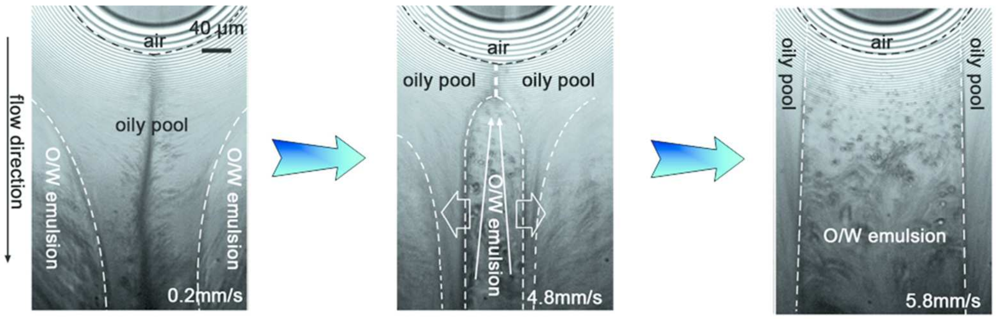

85x27mm (300 x 300 DPI)

Direct observation of formation and destruction of the inversed continuous oil phase in the micro outlet region achieved by the confined diluted O/W emulsion stream

Liran Ma[1]*, Xuefeng Xu[2], Chenhui Zhang[1], Jianbin Luo[1]

1 State Key Laboratory of Tribology, Tsinghua University, Beijing, 100084, China.

2 School of Technology, Beijing Forestry University, Beijing 100083, China

E-mail: maliran@tsinghua.edu.cn

Abstract

We demonstrate a direct observation of the oil-in-water (O/W) emulsion droplets in confined point contact geometry, extending earlier studies to shed new light on the mechanism of the interaction between emulsion and solid surfaces under confinement. Significantly, the behavior of droplets at the outlet of the contact area is highlighted. The interference technique offers capabilities to distinguish different phase of liquid based on the divisive refractive indices. A continuous oil phase can be initially obtained surrounding the contact area, at both the inlet and outlet, as a result of the confinement-induced phase inversion, which has been recognized as the efficient reservoir to the contact. However, in the outlet region, such reservoir is observed to be readily destroyed by the back flow of the diluted bulk emulsion, resulting in a notable coexistence of both the O/W and W/O phases in several distinguishing microscopic zones adjacent to each other. This suggests that the breakup of the reservoir may underlie the limited absorption and lubricity of diluted O/W emulsion systems.

Keywords: emulsion droplet; confinement; outlet; backflow; inversion

1. Introduction

Emulsions, with one liquid phase dispersed in the other one, have been recognized as a routine part of our lives, to be useful in a wide range of applications. Oil-in-water (O/W) emulsions with oil droplets dispersed in bulk water have been extensively used in many fields, such as food, pharmaceutics, and manufacturing and so on [1-3]. Although the behavior of O/W emulsions has received a high degree of attention in the last several decades, the way emulsions response to solid surfaces still elicits wonder, which will be of great importance in both scientific and industrial applications. As controlling emulsion flow behavior and stability is critical [4], the effects of the gap between the walls on the droplet behavior are recognized to be crucial from both academic and industrial perspectives. Typically, the emulsion systems confined in a small gap with similar or smaller size of the droplet have been extensively studied due to the rapidly developing microscale technologies in the past several decades [5-7].

There have been many remarkable phenomena reported [8, 9] for microfluidic devices and applications. Migler and co-workers [10, 11] have reported the transition of emulsion droplets to strings in polymeric emulsions, resulted from the coalescence when sheared between parallel plates with microgap. Dilute emulsions have been reported to behave like viscous liquids under confinement [12, 13], and the breakup of the droplets can be easily observed [14, 15]. While, concentrated emulsions were found to show a transition from a fluid to a solid-like material in narrow confined gap [16-18].

To target different applications, the behavior of emulsions through a wedgelike gap is of special importance and interests in some cases, typically, lubrication and metal processing [19, 20]. As to the O/W emulsions, a phase inversion has been recognized to come into being with the flow towards the contracted gap, as a result of the concentration of the oil droplets [21-23]. In our previous work [24-26], we observed such inversion directly in a wedgelike gap formed by the inlet of a ball on disc contact geometry, and systematically demonstrated the influence factors, which was also confirmed to be related to the film formation ability of emulsions. The lubricity of diluted O/W emulsion has been recognized to be significantly limited in contrast to pure oil, in spite of the concentration and inversion formed ahead of the contact [21-24]. The mechanism is still dubious. Thus, it would be of interest to take a further view of the outlet of a ball on disc contact geometry, which has been seldom reported. In the present work, we disperse droplets of paraffin oil in a continuous phase of water. There is an emphasis on the direct observation of the behavior of emulsion droplets. The formation and destruction of emulsion phase inversion induced by the flow and confinement at the outlet of contact was studied. Then, the effects of oil concentration, emulsifier and rolling speed were discussed in detail, which could help to take a deep view of the mechanism of the oil-in-water emulsion in confinement.

2. Experimental

The experimental set-up used has been described earlier [28] in detail and is shown schematically in Figure 1. The ball-on-disc geometry was obtained by using a highly polished steel ball with diameter of 22.225mm and surface roughness Ra of 3.7nm (purchased from Amatsuji Steel Ball Mfg. Co. Ltd, Osaka, Japan) under a semi-reflective chromium coated highly polished glass disc with a surface roughness Ra of around 0.5nm, under pure rolling conditions. The steel ball is half-submerged in emulsion. A monochrome camera and a microscope with the light incoming vertically were utilized to capture the pictures of emulsion droplets behavior nearby the contact area. Experiments are conducted under a maximum contact pressure of approximately 0.5GPa, at a room temperature of 25±1°C. Purified water with a resistivity of 18.2MΩ (produced by Thermo TKA purification system, MA, U.S.), was used as the continuous phase. Paraffin oil with a viscosity of 30mPas at 25°C (purchased from Chemical Regent Co., Ltd., Beijing, China), was used as the dispersed phase. Tween 80 and Span 80 were mixed with various a mass ratio of 1:1 to get the hybrid emulsifier with corresponding hydrophilic-lipophilic balance (HLB) value of 9.65, which can result in a relatively good stability in a range of HLB from 7 to 12. The volume ratio of the mixed emulsifier in the oil was changed to study the effect of the emulsifier. 0.5vol% and 5vol% emulsions were prepared for the experiments. Before experiments, all pieces were ultrasonically cleaned using organic solvents and de-ionized water to get rid of the contaminations.

3. Results

In the present work, a simple but effective approach is used to distinguish different phase, such as water, oil and air. We take advantage of the basic interference concept, which can directly demonstrate the interference fringes. Based on the relative optical interference intensity approach (ROII), the optical interference intensity under vertical incidence condition can be expressed as [27]:

$$I = I_1 + I_2 + 2\sqrt{I_1 I_2}\cos\delta = I_1 + I_2 + 2\sqrt{I_1 I_2}\cos(4\pi kh/\lambda + \Phi) \quad (1)$$

where I is the interference intensity, I_1 and I_2 are the intensity of the two interference beams, k is the refractive index of the liquid media, h is the gap size between the two surfaces, λ is the wave length of the incident light, and Φ is the phase change caused by the surfaces of the chromium layer and the steel ball. It can be concluded for the same geometry, the small refractive index will result in a dense fringes distribution. Thus, the media in the confinement can be recognized from the density of the fringes. In our previous work, the existence of an oily pool at the inlet has been confirmed by the refractive index measurement, as a result of the breakup of the droplets induced by the confinement [25, 26].

Our initial measurement in the present work is to study the behavior of 5vol% O/W emulsion at the outlet, with 10vol% volume ratio of the mixed emulsifier in the dispersed oil. As shown in Figure 1, where the circle at the top represents the contact area, the interference fringes is resulted from the coated chromium layer [27, 28], the region at the bottom represents the outlet region, and the flow direction is along with the arrow at the side.

3.1 Formation of a closed oil pool at the outlet

Figure 2 shows the droplet behavior of 5vol% emulsion captured at a speed of 1mm/s, with a successive variation as the time goes by. In Figure 2(a), obviously, a continuous and closed oily pool with a refractive index around 1.48 can be observed to notably exist at the outlet, as highlighted by the broken lines. This inversed oily region surrounding the contact area is resulted from the breakup of the oil droplets when they are moving towards the contact area in the wedge-like gap at the inlet, which is consistent with results reported [25, 26]. At the outlet, as the rolling speed is quite low, the oil-phase streams split by the contact area can easily meet with each other and finally lead to a closed oily pool. In this outlet inversed oily zone, significantly, some small water droplets with various diameters can be observed to distribute nearby the center line of the outlet. The water droplet size varies from small to large along the flow direction. The largest droplet diameter is 8μm, however the smallest droplet could not be measured limited by the microscopy technique in the current system. Most of the measurable droplets are around 2-5μm. As a result, a visible water-droplet-rich centre line along the centre of the contact area at outlet is formed.

To illuminate the movement of the droplets in the oily region, a series of pictures were demonstrated in Figure 2(a) to (h), with time interval of 0.15s. Typically, a droplet nearby the boundary of the oily pool has been found to move towards the center line, as marked by the short arrow. The speed of this droplet can be easily calculated to be around 20μm/s, from the position variation and the time interval from Figure 2(d) to (h). This speed is much lower than the rolling speed of the surfaces. The presence of the water drops here comes from the small fraction of water involved in the inversed oily region.

3.2 Destruction of the oily pool at the outlet iris aperture

As demonstrated in Figure 3, where the effect of oil concentration can be obviously distinguished, the images were captured with 0.5vol% and 5vol% emulsions respectively at the same rolling speed of 1mm/s, with the 10vol% volume ratios of the mixed emulsifier in the oil. In term of the 5vol% emulsion, the oily pool at the outlet region is still maintaining closed, while the one for the 0.5vol% emulsion was cut into several parts by the backflow of the O/W bulk phase. It can be noted in Figure 3(a) that there are mainly five visible zones in the outlet region. To maintain a sufficient supply to the contact and form a closed oily pool at the outlet, sufficient supply of oil should be required. Consequently the opened oily pool at the outlet achieved by using 0.5vol% can be attributed to the insufficiency of oil amount. Moreover, the presence of the closed oily pool as shown in Figure 3(b) is actually calling for both sufficient oil and a rapid response of the liquid to replenish the contact track, which will be significantly affected by the viscosity of the liquid and the rolling speed of the solid surfaces. Taking the solid-like material as example, the rolling track will be unable to be replenished, inducing a broken oily pool at the outlet. As to the situation of relatively high speed, when there is no enough time for the liquid to recover the contact track, an opened oily pool will also come into being at the outlet of the contact.

We are focusing on the patterns arising for the increasing speed in the present work, to take a view of the effect of rolling speed. Figure 4(a)-(i) shows the critical variation arising at the outlet region during the speeding up process. The rolling speed of the contact is ranging from 0.2mm/s to 16.4mm/s. The broken line indicates the boundary of different phases. The formation of the air zone close to the contact area has been recognized to be resulted from the pressure distribution in a hydrodynamic flow condition [29]. We are focusing on the breakup of the inversed oily pool at the outlet in the present work. As demonstrated in Figure 4(c), when the speed is approximately 4.8mm/s, the initial inversed oily pool is observed to be cut along the center line into two parts, by the backflow of the bulk O/W emulsion. At the same time, numerous oil droplets flow back into the rolling track and towards the contact area, indicated by the long arrows in Figure 4(c). The short and empty arrows in Figure 4(c) indicate this tendency of this breakup. Thus, this breakup tendency enables the formation of the microscopic multi-phase region, including air zone, O/W emulsion phase and W/O emulsion phase, which have been clearly and typically demonstrated in Figure 4(c). Figure 4(c) to (f) show the rapid variation process caused by the backflow of the O/W bulk emulsion. Typically, in Figure 4(f), when the rolling speed is 5.6mm/s, the boundary of the backflow track starts to stabilize, indicated by the broken lines which can be also observed in the following images Figure 4(g)-(i). Large amount of oil droplets are found to be concentrating, swarming and accumulating in the backflow track. It can be also observed that the droplets with different sizes are well distributed along the centre line, with decreasing diameters when moving towards the contact area, as shown in Figure 4(g)-(i).

4. Discussions

4.1 Distribution of droplet size along the centre line of the outlet

As mentioned in the above section, for both the water droplets in the continuous oil phase and the oil droplets in the backflow continuous water phase, progressive droplet sizes have been notably found along the centre line of the outlet with the direction away from the contact area. To clearly show such phenomena, the droplet size variations are plotted against the position along the centre line of the outlet in Figure 5, where the open circles indicate the water droplets in the continuous oil phase at a speed of 1mm/s, and the solid circles indicate the oil droplets in the backflow water phase at a speed of 8.8mm/s. Under both of those two situations, droplets with larger size can be found to be located further from the contact area. The gap size between the two surfaces is also plotted as predicted by the Hertz theory [31]. In our situation, the gap size in the contact area is around several nanometers deduced from the Harmrock Dowson theory [25], which can be negligible, compared to the gap size out of the contact area. When the central film thickness is quite small, the description can be written as:

$$h_1 = h_0 + \frac{4.53\mathrm{p}_0}{\mathrm{E}'\,\mathrm{a}^{1/2}} \cdot \mathrm{b}^{3/2} \approx \frac{4.53\mathrm{p}_0}{\mathrm{E}'\,\mathrm{a}^{1/2}} \cdot \mathrm{b}^{3/2} \quad (1)$$

where the b is the distance from the edge of the contact area to some point on the centre line of the outlet, h_1 is the gap size between the two surfaces at the specific position, h_0 is the gap size in the contact area, p_0 is the contact pressure of the contact area of 0.53GPa, a is the radius of the contact area of 160μm, E*'* is the equivalent modulus of the contact with a value of around 115.36GPa. Thus, it can be inferred that, the droplet size distributions basically meet the geometry of the gap size between the two surfaces.

Moreover, such distribution of the water droplets may be indicative of the centrifugal movement of the water droplets in the oily phase. The deviation of the droplet d' caused by the centrifugal motion has been deduced in our previous work [25], which can be considered to be proportional to the droplet diameter d, expressed as the following equation [25]:

$$d' \propto \frac{\pi}{\eta}(\rho_W - \rho_O) d^2 u \quad (2)$$

where d' is the deviation of a water droplet with diameter of d, η is the viscosity of paraffin oil, the ρ_w and the ρ_o are the density values of water and paraffin oil respectively, and u can be considered as the rolling speed of the two surfaces. Thus, when the water droplet is large, it will be located far from the contact area, as mentioned above.

4.2 Basics of the destruction of the continuous oil phase

Destruction of the continuous oil phase at the outlet is significantly due to the backflow of the bulk O/W emulsion, which is supposed to be dominated by the streaming. The situation in our experiments can be approximatively considered as a flow past a circular cylinder with a diameter approximate to the diameter of the oily pool. At around 5mm/s, the oily pool can be found to be with a diameter about 680μm, resulting in a Reynold number of 3.4. As reported, eddy will come into being in the outlet region behind the contact area, resulting in the back flow of the bulk O/W emulsion. In the present work, it has been found that the inversed oily pool can be destroyed by the backflow with a continuous water phase. Thus such breakup can be considered to be realized by overcoming the interface of oil and water. The energy required to for this overcoming process can be equal to the oil-water interfacial adhesive energy, which can be expressed as [32]:

$$W_{ow} = 2\sigma_{ow} \tag{3}$$

where W_{ow} is the oil-water interfacial adhesive energy, and σ_{ow} is the oil-water interfacial tension, the value of which will be dominated by the content and type of the emulsifier. We are focusing on the content of the emulsifier in the current system. When there is no emulsifier, the energy required to break the oil pool can be taken as 102.6mN·m^{-1}, which is twice of the oil-water intension of 51.3mN·m^{-1} [25]. Moreover, the motion energy of the backflow required to overcome the oil pool should be equal or larger than W_{ow}. Thus, when the oil-water intension is weakened by the effect of emulsifier, the backflow speed required to break the oil pool should be also decreased. The volume ratios of the mixed emulsifier in the oil in the above section are 10vol%. As demonstrated in Figure 4, for 5vol% O/W emulsion, the breakup speed is around 4.8mm/s-5.6mm/s. This value can be expected to be variable when the concentration of emulsifier is varied. Several ratios of the mixed emulsifier in dispersed oil phase below the critical micelle concentration, 0vol%, 1vol%, 5vol%, 10vol% and 20vol%, are taken to discuss the effect of emulsifier, as shown in Figure 6. Notably decreased breakup speed can be found. It can be indicated that the interface tension between oil and water phases is playing an important role during the breakup process. It can be suggested that the backflow of the bulk diluted emulsion will be a destruction of the oil recovery of the contact track.

It should be noted that the observation of formation and destruction of the oily phase at outlet of the contact area will not only help to reveal the microscopic behavior of emulsion droplets under confinement, but also can shed a new light on the mechanism of the lubrication of emulsion.

5. Conclusions

In the present work, the behavior of diluted O/W emulsions in wedge-like confinement has been investigated. A phase inversion with continuous oily pool has been observed to existence in the outlet region. The pattern of such inversion was found to be significantly affected by the oil volume fraction, a closed oily pool for 5vol% emulsion and a broken one for 0.5vol% emulsion. During the speeding up process, breakup of the oily pool can be notably observed, resulting in the coexistence of O/W and W/O phases in a microscopic region. Thus formation and destruction of the inversed continuous oil phase in the micro outlet region achieved by the confined diluted O/W emulsion stream has been observed.

Acknowledgements

The work was financially supported by the National Natural Science Foundation of China (51305225), the National Key Basic Research Program of China (2013CB934200), Research Fund of the Tsinghua Univeristy (20131089320).

References

1 P. A. Reynolds, M. J. Henderson, S. A. Holt and J. W. White, *Langmui*r, 2002, **18**, 9153.

2 J. Fattaccioli, J. Baudry, N. Henry, F. Brochard-Wyartb and J. Bibettea, *Soft Matter*, 2008, **4**, 2434.

3 S. W. Zhang, *Friction* **1**(2), 2013, 186–194.

4 C. P. Whitby, R. McVicker, J. N. Connor and R. Sedev, *Soft Matter*, 2013, **9**, 5975.

5 J. Happel and H. Brenner, *Low Reynolds Number Hydrodynamics* Nijhoff, The Hague, 1983.

6 H. A. Stone and S. Kim, *AIChE J.* 2001, **47**, 1250.

7 G. M. Whitesides and A. D. Stroock , *Phys. Today* 2001, 42.

8 K. B. Migler, *Phys. Rev. Lett.*, 2001, **86**, 1023.

9 D. R. Link, S. L. Anna, D. A. Weitz and H. A. Stone, *Phys. ReV. Lett.*, 2004, **92**, 0545031.

10 A. S. Utada, E. Lorenceau, D. R. Link, P. D. Kaplan, H. A. Stone and D. A. Weitz, *Science*, 2005, **308**, 537.

11 K. B. Migler, *Phys. ReV. Lett.*, 2001, **86**, 1023.

12 J. A. Pathak and K. B. Migler, *Langmuir*,2003, **19**, 8667.

13 S. Navardi and S. Bhattacharya, *J. Chem. Phys.*, 2010, **11**, 114114.

14 P. A. Kottke, A. Saillard and A. G. Fedorov, *Langmuir*. 2006, **22**(13), 5630.

15 S. Wang, W. Qin, Y. Y. Dai, *Chin. J. Chem. Eng.*, 2012, **20**(2), 239.

16 A. Vananroye, P. Van Puyvelde and P. Moldenaers, *Langmuir*,2006, **22**, 3972.

17 V. Trappe and D. A. Weitz, *Phys. Rev. Lett.*, 2000, **85**, 449.

18 N. D. Denkov, S. Tcholakova, K. Golemanov and A. Lips, *Phys. Rev. Lett.*, 2009, **103**, 118302.

19 M. Clusel, E. I. Corwin, A. O. N. Siemens and J. Brujic, *Nature*, 2009, **460**, 611.

20 R. W. Belfit and N. E. Shirk, *Lubr. Eng.* 1961, **17**, 173.

21 J. C. Whetzel, Jr. and S. Rodman, *Iron Steel Eng.*, 1959, **36**, 123.

22 S. R. Schmid and W. R. D. Wilson, *Lubr. Eng.*, 1996, **52**, 168.

23 T. M. Nakahara, T. Makino and K. Kyogoku, *ASME J. Tribol.*, 1988, **110**, 348.

24 H. X. Yang, S. R. Schmid, R. A. Reich and T. J. Kasun, *J. Tribol.-Trans. ASME*, 2006, **128**, 619.

25 L. R. Ma, J. B. Luo and C. H. Zhang, *Soft matter*, 2011, **7**, 4207.

26 L. R. Ma, C. H. Zhang and J. B. Luo, *Appl. Phys. Lett.*, 2012, **101**, 241603.

27 L. R. Ma, X. F. Xu, C. H. Zhang, D. Guo and J. B. *J. Colloid Interface Sci.*, 2014, **417,** 238.

28 L. R. Ma and C. H. Zhang, *Tribol. Lett.*, 2009, **36**, 239.

29 J.B. Luo, S.Z. Wen and P. Huang, *Wear*, 1996, **194**, 107).

30 S. Z. Wen, Principle of Tribology, Beijing, Tsinghua University Press, 1990.

31 Chiu Y P. An analysis and prediction of lubricant film starvation in rolling contact systems. ASLE Trans, 1974, **17**, 22.

32 D. Myers, Surfaces, in: Interfaces and Colloids—Principles and Applications, 2nd edn, Wiley-VCH, New York, 1999.

Figure caption

Figure 1 Schematic illustration of the experimental setup.

Figure 2 The pictures of the outlet region at a rolling speed of 1mm/s using 5vol% emulsion with 10vol% emulsifier at different time, (a)0s, (b)0.15s, (c)0.30s, (d)0.45s, (e)0.60s, (f)0.75s, (g) 0.90s, (h)1.05s. The broken lines show the boundary of the inversed oily region. The solid line represents the center line of the outlet region. The short arrow indicates the movement of a typical water droplet. The long arrow indicates the flow direction.

Figure 3 The images captured at the outlet region using (a)0.5vol% and (b)5vol% emulsions with 10vol% emulsifier at a speed of 1mm/s.

Figure 4 Images of the outlet region captured at different rolling speed using 5vol% emulsion with 10vol% emulsifier. (a)0.2mm/s, (b)3.6mm/s, (c)4.8mm/s, (d)5.4mm/s, (e)5.6mms/, (f)5.8mm/s, (g)6.4mm/s, (h)8.8mm/s, (i)16.4mm/s.

Figure 5 Droplet size distributions at outlet along the centre line of the contact area using 5vol% emulsion with 10vol% emulsifier. The open squares indicate the situation of water droplets dispersed in oily pool at 1mm/s. The solid squares indicate the situation of oil droplets in the backflow track at a speed of 8.8mm/s.

Figure 6 Breakup speed of the continuous oily pool at outlet varied with the concentration of emulsifier while the oil concentration is 5vol%.

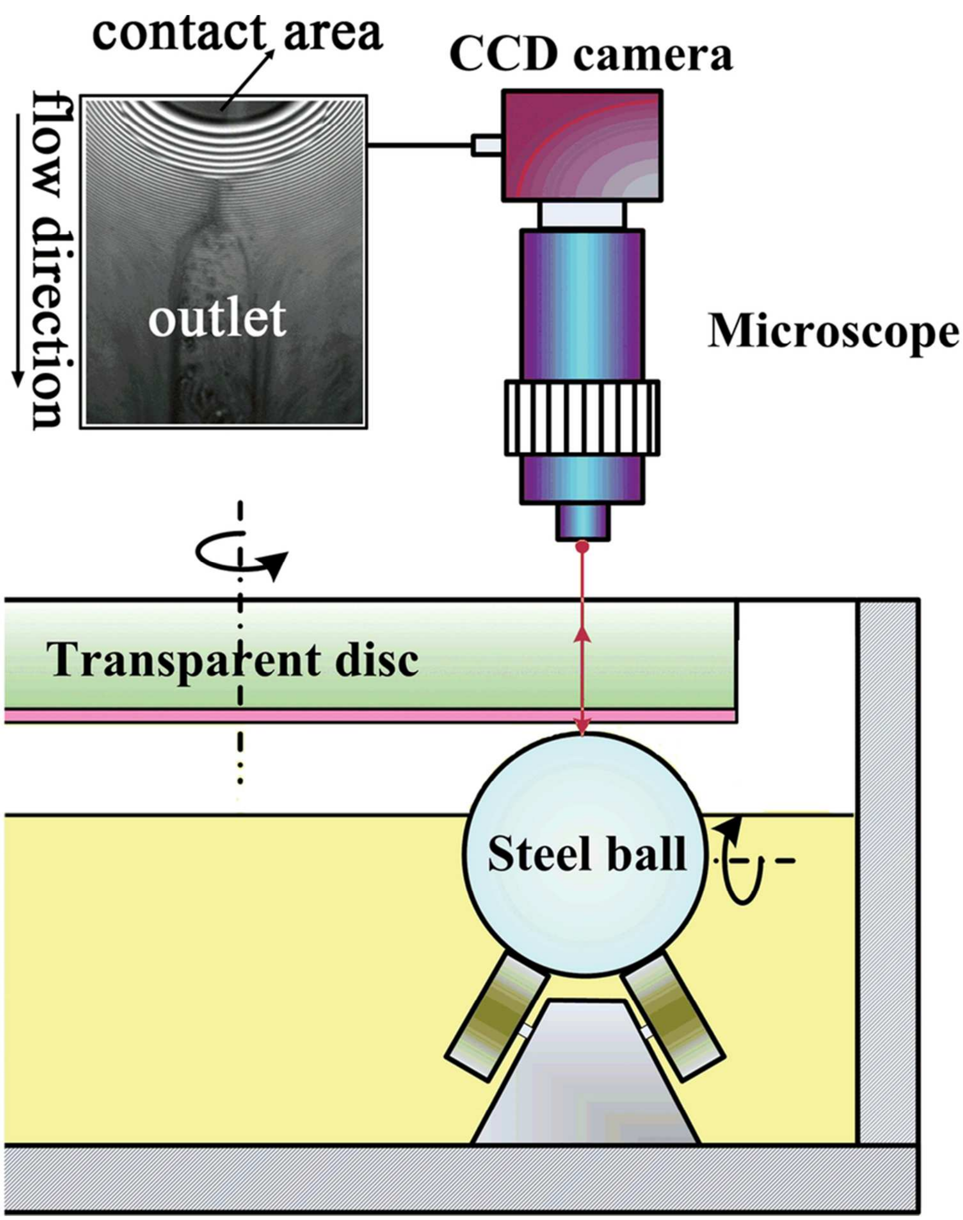

74x91mm (300 x 300 DPI)

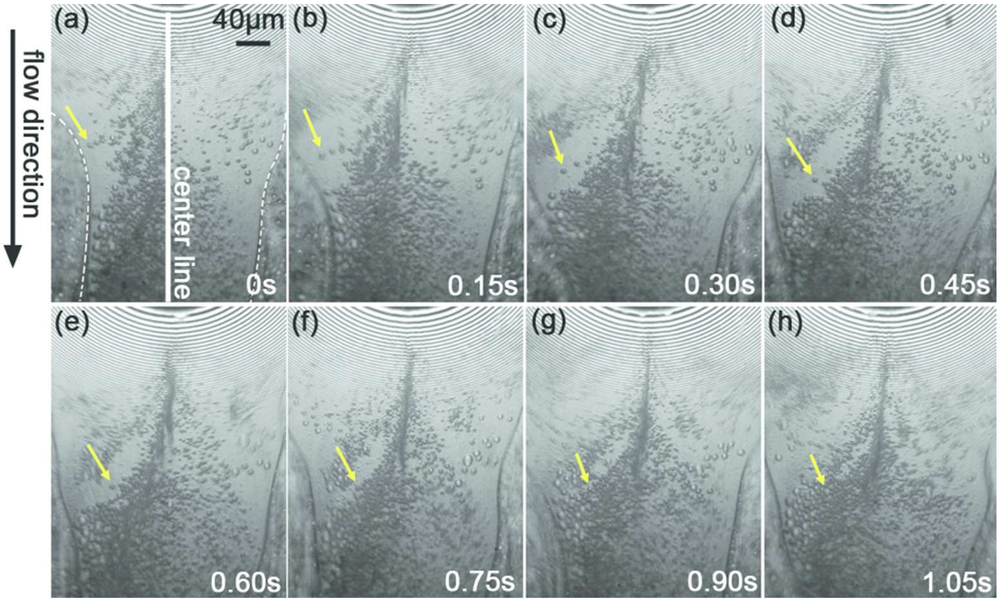

85x50mm (300 x 300 DPI)

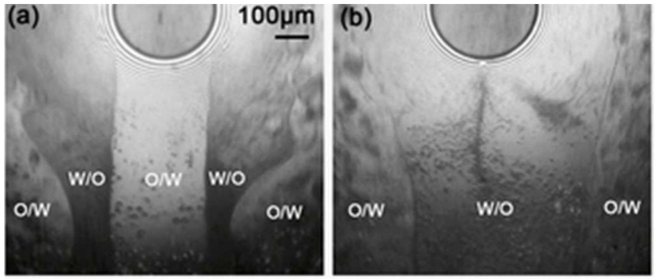

27x11mm (300 x 300 DPI)

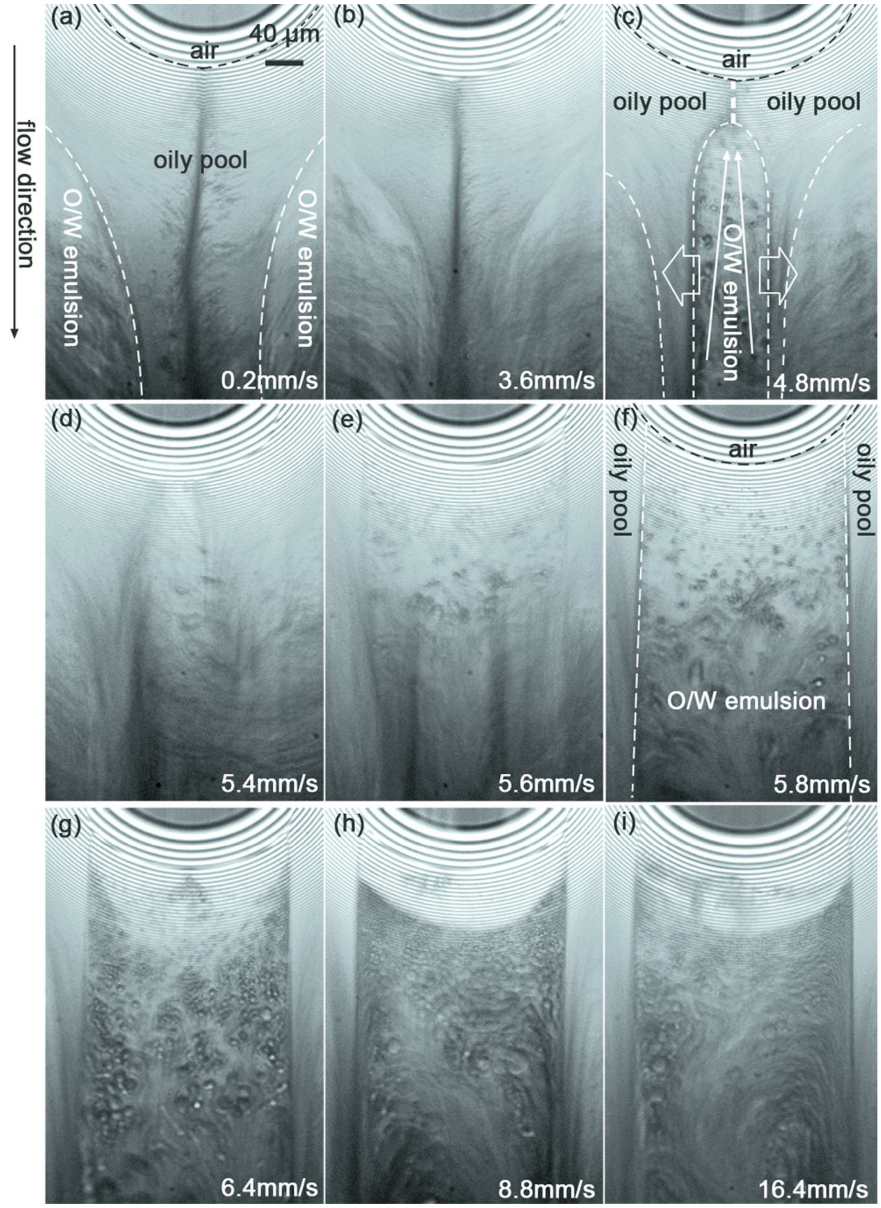

85x115mm (300 x 300 DPI)

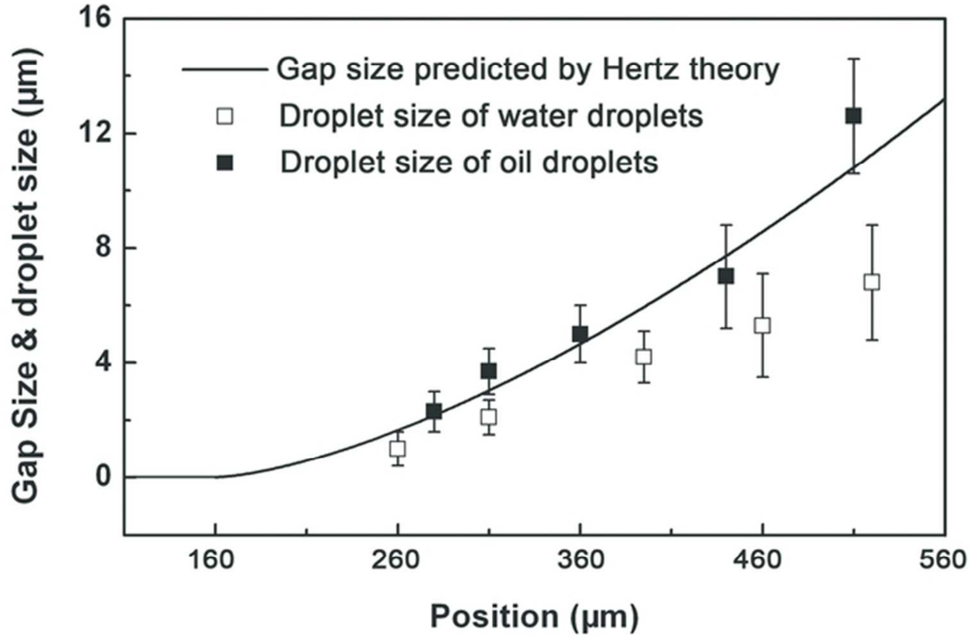

58x40mm (300 x 300 DPI)

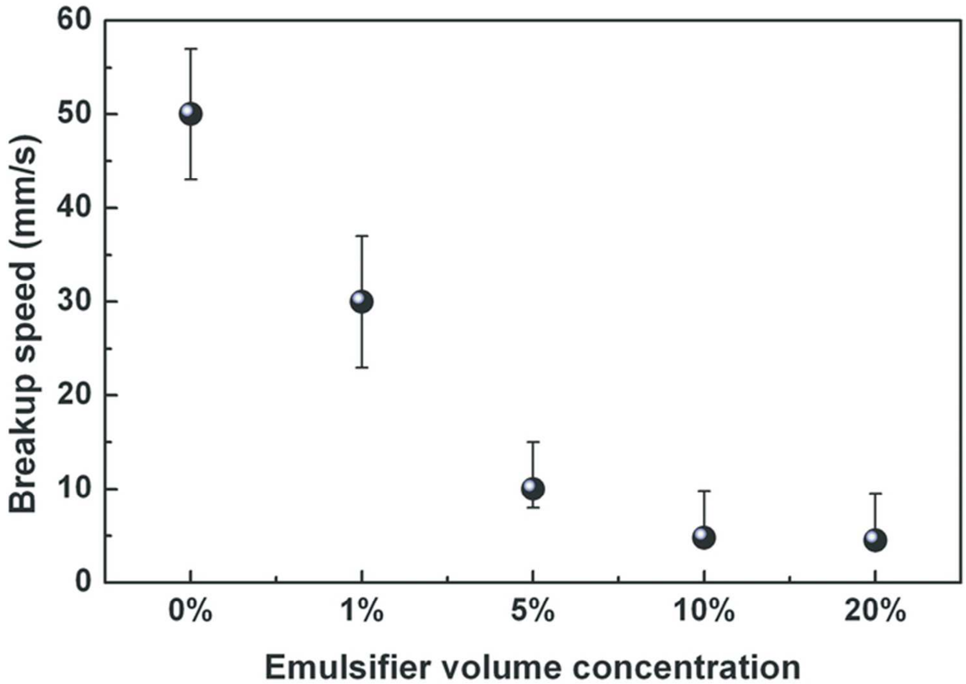

62x46mm (300 x 300 DPI)